Available online at www.sciencedirect.com
SCIENCE DIRECT®
Biochimica et Biophysica Acta 1611 (2003) 63–69
BIOCHIMICA ET BIOPHYSICA ACTA
BBA
www.bba-direct.com

Application of purging biotinylated liposomes from plasma to elucidate influx and efflux processes associated with accumulation of liposomes in solid tumors

Vincent W.H. Fung, Gigi N.C. Chiu, Lawrence D. Mayer*

Division of Pharmaceutics, Faculty of Pharmaceutical Sciences, University of British Columbia, Vancouver, BC, Canada
Department of Advanced Therapeutics, British Columbia Cancer Research Center, 601 West 10th Ave., Vancouver, BC, Canada V5Z 1L3

Received 19 August 2002; received in revised form 3 December 2002; accepted 5 December 2002

Abstract

Although small, 100-nm liposomes are known to selectively accumulate in solid tumors, the individual contributions of liposome influx and egress rates are not well understood. The aim of this work was to determine influx and efflux kinetics for 100-nm, 1,2-distearoyl-*sn*-glycero-3-phosphocholine (DSPC)/cholesterol (Chol) liposomes by inducing aggregate formation of biotinylated liposomes upon administering avidin. Injecting 50 μg of neutravidin intravenously to mice that had previously been administered 100 mg/kg DPSC/Chol liposomes containing 0.5 mol% biotin-conjugated lipid resulted in >90% elimination of the liposomes from plasma within 1 h. This rapid removal by the reticuloendothelial system (RES) permitted the determination of the tumor efflux kinetics due to negligible tumor influx after neutravidin injection. The tumor efflux rate constant (k_{-1}) was determined to be 0.041 h^{-1} when neutravidin was injected 4 h after liposome injection. This allowed the determination of the tumor influx rate constant (k_1), which under these conditions was 0.022 h^{-1}. Therefore, DSPC/Chol liposomal accumulation, in LS180 solid tumors, is dictated primarily by plasma liposome concentrations and liposome egress is comparable or slightly faster than influx into the tumors. This method is applicable for a wide range of lipid doses, and can be used to characterize influx and efflux parameters at different time points after accumulation. The application, therefore, has the potential to be used to fully characterize the impact of different liposome parameters such as lipid composition, steric stabilization, size and dose on tumor accumulation kinetics.

Keywords: Liposome; Drug delivery; Tumor accumulation; Pharmacokinetics; Biotin–avidin technology

1. Introduction

Liposomes have been widely employed as carrier systems for anticancer drugs and other agents. It is well established that liposomes accumulate preferentially in disease sites, including tumors due to increases in tumor blood vessel permeability [1–3]. However, little is known about the detailed kinetic properties underlying liposome accumulation in tumors. In particular, the relative contribution of tumor influx and efflux of liposomes to the overall tumor accumulation phenomenon has not been elucidated. Moreover, due to conflicting results arising from recent studies that question the beneficial effects of liposome formulations with extended half-lives [4–6], it has become increasingly important to characterize the detailed mechanisms underlying tumor accumulation of liposomes.

Previous studies have described methods to clear liposomes from the blood compartment to increase target-to-blood ratios for rapid diagnostic imaging [7–9]. In this approach, liposomes containing biotin-derivatized lipids were administered intravenously followed by injection of

Abbreviations: DSPC, 1,2-distearoyl-*sn*-glycero-3-phosphocholine; Chol, cholesterol; CHE, cholesterylhexadecyl ether; RES, reticuloendothelial system; HBS, HEPES buffer saline; Biotin-X-DSPE, *N*-((6(biotinoyl)amino)hexanoyl)-1,2-distearoyl-*sn*-glycero-3-phosphoethanolamine; QELS, quasielastic light scattering; PEG, poly(ethylene glycol); AUC, area under the curve; ANOVA, analysis of variance

* Corresponding author. Department of Advanced Therapeutics, British Columbia Cancer Research Center, 601 West 10th Ave., Vancouver, BC, Canada V5Z 1L3. Tel.: +1-604-708-5836; fax: +1-604-877-6011.
E-mail address: lmayer@bccancer.bc.ca (L.D. Mayer).

0005-2736/03/$ - see front matter © 2003 Elsevier Science B.V. All rights reserved.
doi:10.1016/S0005-2736(02)00704-6

avidin at times sufficient to allow liposome accumulation in the disease site. Aggregates of liposomes formed in the blood due to the high affinity between biotin and avidin ($K_d \cong 10^{-15}$ M) are rapidly recognized and cleared by the reticuloendothelial system (RES), primarily in organs such as the liver, spleen and lungs. However, these prior studies utilized liposome doses for imaging that were approximately 10-fold lower than doses typically used for therapeutic applications. In the present study, we have investigated the use of biotin-labeled liposomes to elucidate the individual contribution of influx and efflux rates to the net accumulation of liposomes in solid tumors. The rapid removal of liposomes provides the possibility of studying tumor efflux in isolation because it eliminates the otherwise interfering influx of liposomes from the circulation (Fig. 1). Liposomes injected into tumor-bearing mice can be allowed to accumulate in the tumor over a chosen time period. The subsequent injection of neutravidin should rapidly clear circulating liposomes, thereby allowing efflux of liposomes from the tumor to be monitored over time. Determination of the efflux rate constants from these data can then allow tumor influx rate constants to be calculated based on known plasma liposome concentrations. We adapted this approach to studying tumor accumulation kinetics by optimizing biotin–lipid content and neutravidin dose for rapid plasma elimination. Tumor efflux and influx kinetics were determined for 100-nm, 1,2-distearoyl-*sn*-glycero-3-phosphocholine (DSPC)/cholesterol (Chol) using the LS180 human colon carcinoma solid tumor xenograft model. Our results have demonstrated the utility of this method in understanding the mechanisms underlying accumulation of liposomes in solid tumors. This information may greatly assist the development of liposomal anticancer drug formulations with improved therapeutic activity.

2. Materials and methods

2.1. Materials

DSPC and Chol were purchased from Avanti Polar Lipids (Alabaster, AL). *N*-((6(biotinoyl)amino)hexanoyl)-1,2-distearoyl-*sn*-glycero-3-phosphoethanolamine (Biotin-X-DSPE) was obtained from Northern Lipids (Vancouver, BC). [^{3}H]cholesteryl hexadecyl ether (CHE) was from Amersham (Oakville, ON). HEPES and hydrogen peroxide were purchased from Sigma Chemical (St. Louis, MO). Neutravidin was obtained from Pierce Chemical (Rockford, IL). Solvable™ was from NEN Research Products (Dupont Canada, Mississauga, ON, Canada). LS180 cells (a human colon carcinoma cell line) were purchased from the ATCC (Manassas, VA) and maintained in culture. CD-1 mice (20–

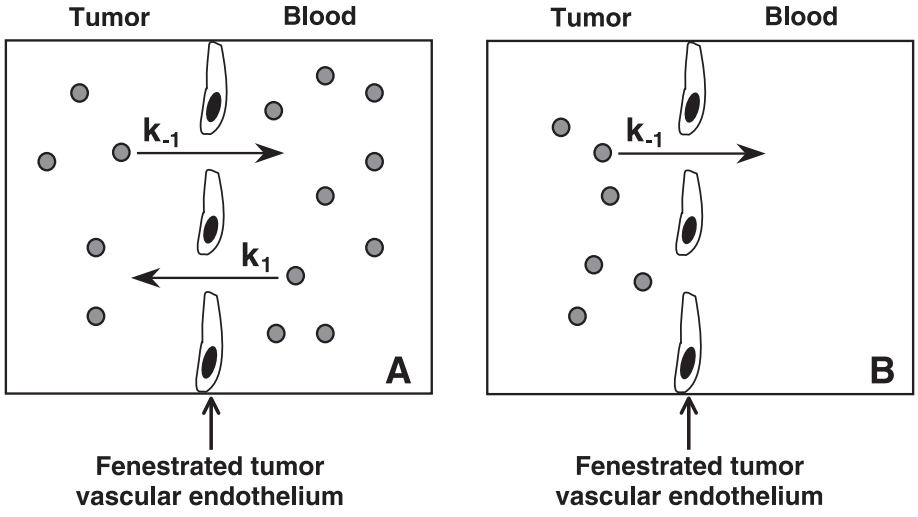

$$\frac{d[L_{tumor}]}{dt} = k_1[L_{blood}] - k_{-1}[L_{tumor}]$$

$$\lim[L_{blood}] \rightarrow 0,\ k_1 \rightarrow 0$$

$$\frac{d[L_{tumor}]}{dt} = -k_{-1}[L_{tumor}]$$

Fig. 1. Influx and efflux contribution of liposomal accumulation. During tumor accumulation of liposomes (gray circles), both influx and efflux take place (A), with rate constants k_1 and k_{-1}, respectively. Rapid clearance of circulating liposomes (B) allows the isolation of a single kinetic variable, tumor efflux, as shown in the accompanying equations, where L_{tumor} represents tumor liposome concentrations and L_{blood} represents blood liposome concentrations.

23 g) and female SCID/RAG2 (25–26 g) were bred from British Columbia Cancer Agency Animal Breeding Facility (Vancouver, Canada).

2.2. Preparation of liposomes

DSPC/Chol/Biotin-X-DSPE (54.5:45:0.5 mole ratio) liposomes were prepared using extrusion technology [10–12]. Lipids were dissolved in chloroform, and trace amount of [^{3}H]CHE was added as a non-exchangeable and non-metabolizable lipid marker before drying down the mixture to a homogenous lipid film under a stream of nitrogen gas [13,14]. This resulting lipid film was placed under high vacuum overnight to remove any residual chloroform. Subsequently, the lipid film was hydrated in 20 mM/150 mM NaCl HEPES buffer (pH 7.5) (HBS) at 65 °C to a final lipid concentration of 100 mg/ml to form multilamellar vesicles. The resulting mixture was frozen in liquid nitrogen and thawed five times followed by extrusion through two stacked 0.08 μm pore size polycarbonate filters (Nuclepore, Pleasanton, CA) using an extrusion device (Northern Lipids, Vancouver, BC, Canada). The size of the liposomes was determined by quasielastic light scattering (QELS) using a Nicomp submicron particle sizer model 370/270 (Pacific Scientific, Santa Barbara, CA) operating at 632.8 nm. The mean diameter of these liposomes was 100 ± 10 nm.

2.3. In vitro aggregation

Liposomes (1 mg) of 100 nm diameter and neutravidin (25 μg) were incubated in a total volume of 750 μl HBS in 1.5 ml eppendorf tubes for 45 min at 37 °C with constant shaking. Aliquots were removed and the size of liposomes was determined by QELS at 5, 15, 30 and 45 min.

2.4. Plasma pharmacokinetics and tissue distribution of liposomes

All in vivo studies were completed using protocols approved by the University of British Columbia's Animal Care Committee, where these studies met the current guidelines of the Canadian Council of Animal Care. Liposomes, labeled with [^{3}H]CHE, were injected intravenously with various lipid doses in 200 μl via the lateral tail vein. At designated times, three mice were anesthetized with CO_2 and whole blood was collected via cardiac puncture and placed into EDTA-coated Microtainers (Becton Dickinson, Lincoln Park, NJ). Plasma was isolated following centrifugation at 4 °C for 15 min at $1000 \times g$. Aliquoted plasma samples (100 μl) were mixed with 5 ml Pico-Fluor 15 (Packard Biosciences, The Netherlands) scintillation fluid for radioactivity counting.

Tissues including liver, spleen, lungs and tumors were harvested and washed in saline and placed into preweighed glass tubes. Tissue weights were determined before freezing the samples at −70 °C. Appropriate volumes of distilled water were added to tissues to achieve a 30% homogenate (w/v) by homogenizing the mixture with a Polytron tissue homogenizer (Kinematica, Lucerne, Switzerland). Aliquots of the homogenate (200 μl) were added to 500 μl Solvable, and the mixture was incubated at 50 °C for 3 h. After cooling to room temperature, 50 μl of 200 mM EDTA, 200 μl of 30% hydrogen peroxide and 25 μl of 10 N HCl were added. The mixture was then incubated for 1 h at room temperature before adding 5 ml scintillation fluid for radioactive counting. All tissue lipid levels were corrected for lipid in the plasma compartment by using predetermined plasma volume correction factors.

2.5. Liposome elimination from plasma via neutravidin administration

To achieve rapid removal of biotinylated liposomes, the effects of different doses of neutravidin on their pharmacokinetics were studied. In the absence of neutravidin, the elimination profile of DSPC/Chol/Biotin-X-DSPE (molar ratio; 54.5:45:0.5) liposomes at a dose of 100 mg/kg was initially studied in CD-1 mice over a 24-h period. Liposomes were quantitated in plasma and various organs at 1, 4 and 24 h as described in Section 2.4.

To examine the effects of neutravidin on the biodistribution changes of biotinylated liposomes, various neutravidin doses were injected into the tail vein at different times after liposome injection. Plasma and various organs were then sampled at the indicated times and liposomal levels were measured as described in Section 2.4.

2.6. Tumor accumulation and plasma elimination studies of biotinylated liposomes with and without neutravidin

Female SCID/RAG-2 mice were inoculated bilaterally with 1×10^6 LS180 cells subcutaneously on the hind regions of the back. Once the tumors reached an estimated mass of 0.5 g, mice were injected intravenously with 100 mg/kg dose of biotinylated liposomes. Tumor and plasma liposomal levels were determined at 1, 2, 4, 8 and 24 h after injection of liposomes. To characterize the effects of neutravidin on tumor and plasma levels of liposomes, neutravidin was administered to mice 4 h post-injection of liposomes. Liposome levels in both tumor and plasma were then quantified at 1, 2, 4, 8 and 24 h after administration of neutravidin. Tumor efflux behavior was then monitored; efflux and influx rate constants were calculated using pharmacokinetic equations and integral calculus.

2.7. Statistical analysis

Analysis of variance (ANOVA) was performed with the statistical software package (Jmp-In. 4.0, Cary, NC) on the results obtained after administration of the three neutravidin doses. Differences were considered significant at $P < 0.05$.

3. Results

3.1. Aggregation by avidin in vitro

Liposome aggregation was initially evaluated in vitro to ensure the incorporation of the biotinylated lipids in the liposome formulation, the accessibility of the biotin moieties on the liposome surface to neutravidin, and the formation of liposome aggregates with neutravidin. The Biotin-X-DSPE lipid used in this study contains an amino-hexanoyl spacer that allows biotin to be extended away from the liposome, thus increasing the exposure of the biotin moiety, compared to biotin–DSPE [15]. Neutravidin was chosen because it has less non-specific binding than that of avidin [16]. These were two modifications made to previous protocols in the hope of achieving more rapid liposome clearance from the bloodstream.

Increases in liposome diameter were observed within 5 min of incubation with neutravidin, changing from a diameter of 100 ± 10 to 380 ± 170 nm. It is important to note that the mean diameter measured by QELS merely serves as an indicator of aggregate formation, and should not be used as an accurate measurement of the aggregate size. Because aggregation is a random process, homogenous formation of aggregates is not expected, which leads to broad size distribution. After 45 min of incubation with neutravidin, the mean diameter of liposomes was 720 nm with S.D. of 500 nm, indicating the heterogeneity and vast number of aggregates present.

3.2. Effects of various doses of neutravidin on plasma elimination and tissue distribution of biotinylated liposomes

The elimination profile of the biotinylated liposomes in CD-1 mice injected with a lipid dose of 100 mg/kg but without neutravidin was examined over a 24-h period. The percentage injected dose remaining in plasma for biotinylated liposomes were 50%, 31% and 5.5% at 1, 4 and 24 h, respectively, whereas the percentage injected dose remaining in plasma for non-biotinylated liposomes were 57%, 28% and 7.3% at 1, 4 and 24 h, respectively. This indicates that the incorporation of biotin-derivatized lipids did not alter the inherent plasma pharmacokinetics of the non-biotinylated liposomal formulation.

One hour after liposome injection, neutravidin was administered to induce rapid clearance of biotinylated liposomes. All three neutravidin doses resulted in at least 95% clearance of liposomes from the plasma within 1 h after injection of the protein (Fig. 2). The lipid levels decreased from a mean of about 1350 μg lipid/g plasma at $t=1$ h to a mean of less than 50 μg lipid/g plasma at $t=2$ h. The cleared liposomes were observed to accumulate in the RES organs. The neturavidin-induced clearance properties exhibited modest dose dependency, with 200 μg neutravidin giving rise to a mean plasma elimination in 1 h of approximately 99%, 98% with 100 μg and 95% with 50 μg neutravidin.

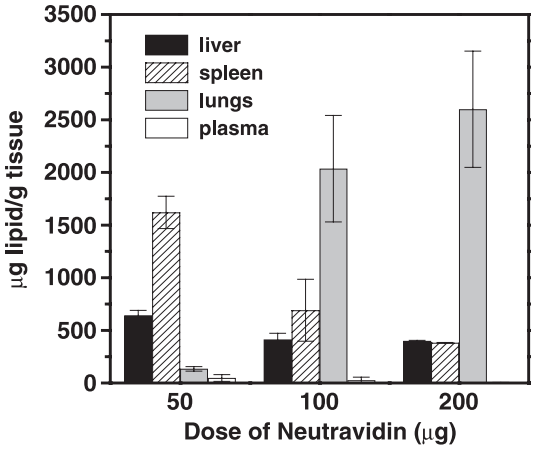

Fig. 2. Biodistribution of DSPC/Chol/Biotin-X-DSPE liposomes with various doses of neutravidin. Biotinylated liposomes (100 mg/kg and 100 nm in diameter) were injected into female CD-1 mice, and various doses of neutravidin were administered (50, 100, 200 μg) 1 h after liposome injection. Liver (black bars), spleen (hatched bars), lungs (gray bars) and plasma (white bars) were quantified for liposomal lipid levels 1 h after neutravidin injection. Each bar represents the mean ± S.D. for three animals.

The differences, however, were not statistically significant (ANOVA, $P>0.05$). Compared to the mice injected with 50 μg neutravidin, the mice with 100 and 200 μg neutravidin were sluggish, tired, and were not as active throughout the 1-h period. This could be attributed to the elevated accumulation of liposomes in the lungs observed for these groups as shown in Fig. 2. In the groups administered with 100 and 200 μg dose of neutravidin, the mean lipid levels in the lungs were approximately 2000 and 2700 μg lipid/g tissue, respectively, compared to a mean lipid level of about 150 μg/g tissue in the group treated with 50 μg neutravidin. Therefore, 50 μg dose of neutravidin was chosen for subsequent experiments to avoid untoward pulmonary reactions.

Mice were sacrificed at 15, 30, 45 and 60 min post-neutravidin administration (50 μg dose) to evaluate the kinetics of neutravidin-induced removal of the liposomes. The removal of liposomes after neutravidin was a rapid process as shown in Fig. 3. More than 70% of lipids were cleared within 15 min, and over 90% were cleared within 1 h.

3.3. Effects of liposomal dose and administration times on neutravidin-induced liposome clearance

In addition to examining the effects of neutravidin on liposomes dosed at 100 mg/kg, a 10 mg/kg lipid dose was also studied to evaluate the versatility and applicability of the rapid neutravidin-based liposome clearance. As shown in Table 1, administration of 50 μg neutravidin resulted in greater than 95% of 10 mg/kg lipid dose eliminated from plasma in 1 h. The effects of administering neutravidin at 4 and 8 h after the initial liposome injection were also

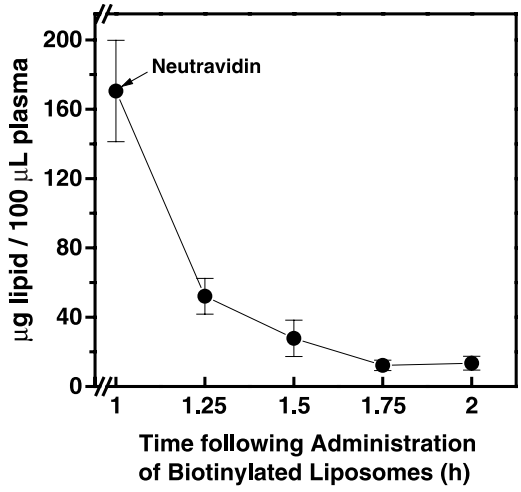

Fig. 3. Plasma elimination of DSPC/Chol/Biotin-X-DSPE liposomes with neutravidin over 1 h. Biotinylated liposomes (100 mg/kg and 100 nm in diameter) were injected into female CD-1 mice. Fifty micrograms of neutravidin was administered 1 h after liposomal injection. Plasma liposomal lipid levels were quantified 15, 30, 45 and 60 min post-injection of neutravidin, as described in Section 2. Each data point represents the mean ± S.D. for three animals.

assessed for the lipid dose of 100 mg/kg. Rapid removal of liposomes was also seen at these time points, with greater than 95% lipid being cleared within 30 min (Table 1). The 30-min time point was chosen to reduce potential false-positive results with neutravidin's effects. This relates to the possibility that a low lipid level at 1 h after neutravidin administration may be related to the lower liposomal lipid concentrations present at $t=4$ and 8 h.

3.4. Liposomal pharmacokinetics in tumor-bearing mice and characterization of tumor efflux and influx

Lipid levels were measured in established LS180 solid tumors and plasma over a 24-h period after a single intravenous injection of biotinylated liposomes (100 mg/kg). In Fig. 4, plasma liposome levels are shown in panel A, and tumor liposome levels are shown in panel B. The plasma levels declined from about 1800 µg lipid/g plasma at $t=1$ h to 1300 µg lipid/g plasma at $t=4$ h, and then slowly dropped to about 500 µg lipid/g plasma at $t=24$ h. Liposomal levels in tumor tissue increased to about 100 µg lipid/g tumor at

Table 1
Percentage removal of plasma liposomal lipid (DSPC/Chol/Biotin-X-DSPE liposomes) in female CD-1 mice after administration of 50 µg neutravidin

Neutravidin-induced liposomal plasma removal (percentage of control)		
Lipid dose (mg/kg)	Time (h)	Percentage removal (S.D.)
100	1[a]	95 (1)
	4[b]	98 (2)
	8[b]	96 (1)
10	1[a]	97 (1)

[a] Plasma levels were taken 1 h after neutravidin injection.
[b] Plasma levels were taken 30 min after neutravidin injection.

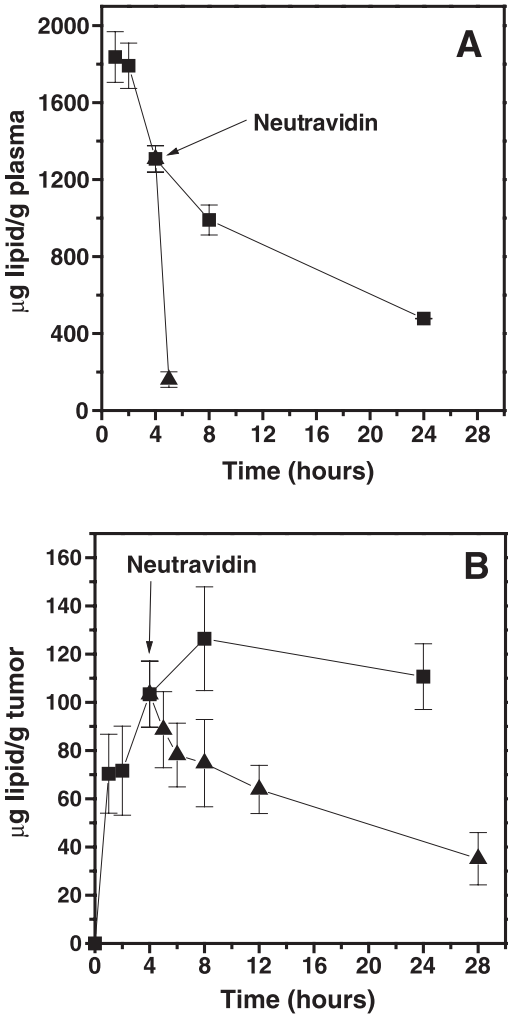

Fig. 4. Plasma elimination and tumor accumulation of DSPC/Chol/Biotin-X-DSPE liposomes with (triangles) and without (squares) administration of neutravidin. Biotinylated liposomes (100 mg/kg and 100 nm in diameter) were injected into SCID/RAG2 mice bearing LS180 solid tumor. Panels A and B represent plasma and tumor liposomal lipid levels, respectively. Tumor and plasma liposomal lipid levels were determined at 1, 2, 4, 8 and 24 h. Fifty micrograms of neutravidin was administered at 4 h after liposome injection, and tumor and plasma liposomal lipid levels were determined at 1, 2, 4, 8 and 24 h after neutravidin administration. Data points represent mean and S.D. from six tumors. Plasma lipid levels were below the limit of quantitation at 6, 8, 12 and 28 h after neutravidin injection.

$t=4$ h, and then peaked at about 120 µg lipid/g tumor at $t=8$ h. The tumor levels appeared to plateau after this time as the levels fell to about 110 µg lipid/g tumor at $t=24$ h. In a matched group of tumor-bearing mice, neutravidin was administered 4 h post injection of liposomes. A rapid decrease in plasma lipid levels was induced, and lipid levels decreased from a mean of about 1300 µg lipid/g plasma at $t=4$ h to <150 µg lipid/g plasma within 1 h. The lipid levels remained below the limit of quantitation (about 10 µg of lipid/g plasma) over the subsequent 23-h period as indicated from the absence of data between $t=6$ h and $t=28$ h in Fig. 4 (panel A). Tumor lipid levels were also observed to gradually

decrease over 24 h after neutravidin addition (Fig. 4, panel B). The levels decreased from 100 μg lipid/g tumor at $t=4$ h to about 30 μg lipid/g tumor at $t=28$ h. The efflux curve was fitted, using the Microcal Origin software package (version 5.0), utilizing the least squares principles which indicates that the efflux curve followed first-order kinetics (Fig. 5). The efflux rate constant (k_{-1}) was then estimated by fitting the curve by a first-order kinetic equation and calculating it from the slope using Eq. (1):

$$\log y = \log y_0 - k_{-1}t/2.303 \quad (1)$$

where y represents tumor liposome concentration at time t, y_0 represents tumor liposome concentration at $t=0$, and k_{-1} represents tumor efflux rate constant for liposomes. From the slope of the fitted curve (see Fig. 5), the tumor efflux rate constant for liposomes (k_{-1}) at $t=4$ h was determined to be 0.041 h^{-1}. Based on the assumption that at any given point in time, the rate of change of tumor lipid levels is equal to the difference between the products of the concentrations in the individual pharmacokinetic compartments and their respective rate constants (see Fig. 1), the influx rate constant (k_1) can be calculated using Eqs. (2) and (3):

$$dy/dt = k_1[C] - k_{-1}[y] \quad (2)$$

where C represents plasma liposome concentration at 4 h. Integrating both sides of Eq. (2) yields Eq. (3):

$$y = (k_1/k_{-1})[C(1 - e^{-k_{-1}t})] \quad (3)$$

Applying the tumor efflux rate constant (k_{-1}) of 0.041 h^{-1}, plasma liposome concentration (C) of 1307 μg/g at 4 h, and tumor liposome concentration (y) of 106 μg/g at 4 h to Eq. (3) yielded a value of 0.022 h^{-1} for k_1.

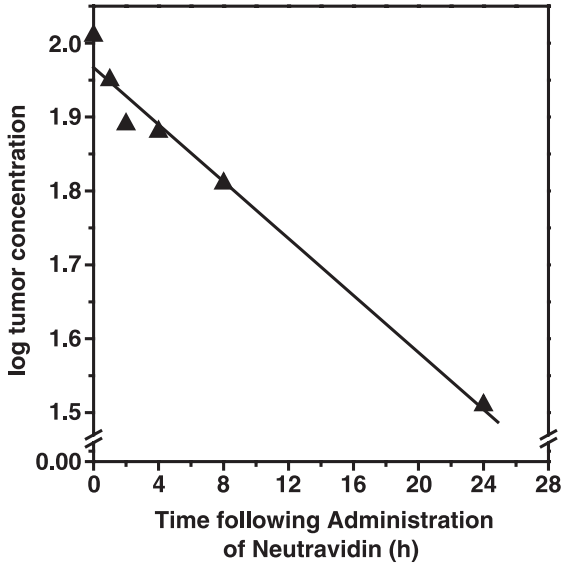

Fig. 5. A plot of the logarithm values of tumor liposome concentrations as a function of the time following neutravidin administration to determine the tumor efflux rate constant, k_{-1}, for biotinylated DSPC/Chol liposomes. Data for tumor liposome concentrations were derived from Fig. 4B. The line was fitted to the data points using Microcal Origin software (version 5.0), and the slope was used to calculate k_{-1}.

4. Discussion

Liposomes have been utilized extensively as drug delivery vehicles for anticancer agents, with several such products approved for therapeutic use in cancer patients. An increasing focus has been placed on designing liposomes with extended circulation longevity, which is believed to improve tumor site delivery through increased plasma liposome concentrations where small, 100-nm liposomes would preferentially extravasate across the leaky vasculature of solid tumors and accumulate to high levels [1–3]. However, modifications to liposome physical properties such as surface-grafted hydrophilic polymers [e.g. poly(ethylene glycol) (PEG)] may possibly alter both influx and efflux rates that contribute to the net flux, or accumulation, of liposomes in solid tumors. Furthermore, liposome influx and efflux rates may be differentially affected by such formulation changes. In this study, we utilized avidin cross-linking of liposomes to rapidly deplete liposomes from the blood compartment, thereby allowing the determination of liposome tumor efflux and influx rates. We have evaluated this methodology to establish its utility in characterizing the detailed tumor accumulation properties of liposomal drug delivery systems.

Other laboratories have employed avidin-induced removal of circulating liposomes to improve target-to-background ratio for imaging and diagnostic purposes [7–9]. Our aim was to optimize the clearance properties to study the kinetics of liposome efflux and influx in solid tumors. It is important to elucidate these variables because accumulation levels in the tumor (in both absolute and dynamic terms) are dependent on the combination of these processes. A low maximum tumor accumulation value may indicate a high efflux and/or slow influx, and vice versa. Consequently, we believe that plasma levels are neither the most accurate predictor nor the ultimate governing factor for tumor levels, and that a detailed pharmacokinetic characterization such as that presented here will help to elucidate the effect of specific liposome properties on tumor uptake properties.

At any point in time during tumor accumulation, both processes of influx and efflux occur simultaneously, making it difficult to determine the individual variables. Rapid removal of liposomes from the circulation, however, permits the isolation and thus the characterization of a single kinetic variable—tumor efflux, by eliminating the otherwise interfering influx factor that is due to accumulating liposomes from plasma (Fig. 1). Unlike other studies that simply aim to obtain a relative improvement in clearance [7–9], rapid clearance is crucial in the present study as we do not want tumor influx to obscure efflux monitoring. It is shown from our results that after neutravidin injection, plasma levels remain minimal throughout the efflux process, and thus

there is minimal interference from the influx process. The present study has successfully achieved rapid elimination of DSPC/Chol liposomes of 100 nm in size and lipid doses of 10 and 100 mg/kg by incorporating 0.5% of Biotin-X-DSPE in the formulation and by administering 50 μg neutravidin.

One concern about the methodology described here is the extravasation of neutravidin into the tumor compartment leading to subsequent interaction with the biotinylated liposomes. We acknowledge that this possibility cannot be ruled out. However, the pool of liposomes in the blood compartment is much higher relative to that in tumor tissues, and this increases the likelihood of quicker access and binding of liposomes to neutravidin, thus minimizing the amount of neutravidin that can access the tumor site. If aggregates do form, they may have difficulty in effluxing out, based on the vascular pore cutoff size (380–780 nm) of the tumor microvessels [17]. The result would be a smaller pool of extravasated, "monomeric" liposomes available for effluxing back out into the blood compartment, and multiphasic efflux kinetics would have been predicted, which is not what we observed. Another concern is the interaction of neutravidin remaining in circulation with the effluxed liposomes. From a previous study, the plasma elimination of neutravidin was rapid, where 50% of injected neutravidin was removed within 30 min [18]; therefore, the likelihood of neutravidin interacting with the liposomes that have effluxed back to circulation would be relatively low. Furthermore, the pool of effluxed liposomes is relatively small, which would also limit their interactions with the remaining neutravidin (already low in plasma levels).

Using the LS180 solid tumor model, we characterized the tumor efflux of liposomes at 4 h after tumor accumulation. The efflux profile, by itself, can be used graphically for comparisons, for example, by overlapping two different efflux curves of interest and qualitatively making comparisons between them. A more quantitative measure is the tumor influx (k_1) and efflux (k_{-1}) rate constants that were also determined in this study. The influx and efflux rate constants were calculated to be 0.022 and 0.041 h^{-1}, respectively, at 4 h after accumulation in LS180 tumors. These rate constants can provide insights to the influx and efflux processes, and can serve as comparators for other tumor models and/or liposome formulations. It is important to note that the rate constants are estimates, given the variability involved in the animal studies, and that the data pertain to the 0–4 h time frame. Thus, this approach may be useful in determining liposome influx and efflux kinetics properties at different times post injection. In the present study, the efflux rate constant was elevated by approximately 2-fold over the influx rate constant. This is consistent with the high hydrostatic pressure that exists in solid tumors [19,20].

The results presented here demonstrate the utility of the plasma liposome quenching method in characterizing the detailed tumor accumulation kinetics of liposomes. This model can potentially serve as a very useful, versatile tool for characterizing and comparing tumor accumulation kinetics of numerous combinations of liposome parameters and tumor models. The pharmacokinetics of different lipid formulations, different doses and even different liposome sizes in various tumor models can be studied. This application allows a better understanding of the mechanisms underlying accumulation of liposomes in tumor, and may be useful in optimizing therapeutic liposome formulations designed to treat solid tumors.

Acknowledgements

We were grateful to Dana Masin, Rebecca Ng, Hong Yan and Sophia Tan for their technical assistance in the animal studies. This research project is supported by a research grant from the Canadian Institute of Health Research. V.F. and G.C. are supported by a graduate fellowship from the University of British Columbia.

References

[1] L.D. Mayer, L.C. Tai, D.S. Ko, D. Masin, R.S. Ginsberg, P.R. Cullis, M.B. Bally, Cancer Res. 49 (1989) 5922–5930.
[2] N.Z. Wu, D. Da, T.L. Rudoll, D. Needham, A.R. Whorton, M.W. Dewhirst, Cancer Res. 53 (1993) 3765–3770.
[3] F. Yuan, M. Leunig, S.K. Huang, D.A. Berk, D. Papahadjopoulos, R.K. Jain, Cancer Res. 54 (1994) 3352–3356.
[4] L.D. Mayer, G. Dougherty, T.O. Harasym, M.B. Bally, J. Pharmacol. Exp. Ther. 280 (1997) 1406–1414.
[5] M.J. Parr, D. Masin, P.R. Cullis, M.B. Bally, J. Pharmacol. Exp. Ther. 280 (1997) 1319–1327.
[6] R.L. Hong, C.J. Huang, Y.L. Tseng, V.F. Pang, S.T. Chen, J.J. Liu, F.H. Chang, Clin. Cancer Res. 5 (1999) 3645–3652.
[7] I. Ogihara-Umeda, T. Sasaki, H. Nishigori, Eur. J. Nucl. Med. 20 (1993) 170–172.
[8] I. Ogihara-Umeda, T. Sasaki, H. Toyama, K. Oda, M. Senda, H. Nishigori, Cancer Res. 54 (1994) 463–467.
[9] I. Ogihara-Umeda, T. Sasaki, H. Toyama, K. Oda, M. Senda, H. Nishigori, Cancer Detec. Prev. 21 (1997) 490–496.
[10] M.J. Hope, M.B. Bally, G. Webb, P.R. Cullis, Biochim. Biophys. Acta 812 (1985) 55–65.
[11] L.D. Mayer, M.J. Hope, P.R. Cullis, A.S. Janoff, Biochim. Biophys. Acta 817 (1985) 193–196.
[12] L.D. Mayer, M.J. Hope, P.R. Cullis, Biochim. Biophys. Acta 858 (1986) 161–168.
[13] J.T. Derksen, H.W. Morselt, G.L. Scherphof, Biochim. Biophys. Acta 931 (1987) 33–40.
[14] M.B. Bally, L.D. Mayer, M.J. Hope, R. Nayar, in: G. Gregoriadis (Ed.), 2nd ed., Liposome Technology, vol. 3, CRC Press, Boca Raton, FL, 1993, pp. 27–41.
[15] P. Corley, H.C. Loughrey, Biochim. Biophys. Acta 1195 (1994) 149–156.
[16] Y. Hiller, J.M. Gershoni, E.A. Bayer, M. Wilchek, Biochem. J. 248 (1987) 167–171.
[17] S.K. Hobbs, W.L. Monsky, F. Yuan, W.G. Roberts, L. Griffith, V.P. Torchilin, R.K. Jain, Proc. Natl. Acad. Sci. U. S. A. 95 (1998) 4607–4612.
[18] Y.S. Kang, Y. Saito, W.M. Pardridge, J. Drug Target. 3 (1995) 159–165.
[19] Y. Boucher, R.K. Jain, Cancer Res. 52 (1992) 5110–5114.
[20] R.K. Jain, in: B.A. Teicher (Ed.), Drug Resistance in Oncology, Marcel Dekker, New York, 1993, pp. 87–105.